INL/JOU-22-70202-Revision-0

Sustainable bioleaching of lithium-ion batteries for critical metal recovery: Process optimization through design of experiments and thermodynamic modeling

December 2023

Majid Alipanah, Hongyue Jin, Qiang Zhou, David Gazzo, Jiangping Liu, Andre Anderko, David W Reed, Vicki S Thompson, Yoshiko Fujita, Caitlin Ann Barboza

INL/JOU-22-70202-Revision-0

Sustainable bioleaching of lithium-ion batteries for critical metal recovery: Process optimization through design of experiments and thermodynamic modeling

Majid Alipanah, Hongyue Jin, Qiang Zhou, David Gazzo, Jiangping Liu, Andre Anderko, David W Reed, Vicki S Thompson, Yoshiko Fujita, Caitlin Ann Barboza

December 2023

Idaho National Laboratory
Idaho Falls, Idaho 83415

http://www.inl.gov

Prepared for the
U.S. Department of Energy
Under DOE Idaho Operations Office
Contract DE-AC07-05ID14517

Sustainable Bioleaching of Lithium-ion Batteries for Critical Metal Recovery: Process Optimization through Design of Experiments and Thermodynamic Modeling

Majid Alipanah[1], Hongyue Jin[1], Qiang Zhou[1], Caitlin Barboza[2], David Gazzo[2,4], Vicki Thompson[2], Yoshiko Fujita[2], Jiangping Liu[3], Andre Anderko[3], David Reed[2]*

[1]Critical Materials Innovation Hub, Department of Systems and Industrial Engineering, University of Arizona, 1127 E. James E. Rogers Way, Tucson, Arizona, 85721, United States

[2] Critical Materials Innovation Hub, Idaho National Laboratory, P.O. Box 1625, Idaho Falls, Idaho, 83415-2203, United States

[3]Critical Materials Innovation Hub, OLI Systems, Inc., 2 Gatehall Dr., Suite 1D, Parsippany, New Jersey, 07054, United States

[4]Department of Chemical and Biomolecular Engineering, University of Notre Dame, 250 Nieuwland Hall, Notre Dame, Indiana, 46556, United States

[*] Corresponding author. Tel.: 1 520-621-7284. E-mail: hjin@arizona.edu

ABSTRACT

Recycling spent lithium-ion batteries (LIBs) could alleviate supply risks for critical metals and be less harmful to the environment compared to new production of metals from mining. Developing a cost-effective LIB bioleaching process could be a promising alternative to traditional energy-intensive recycling technologies. This study aimed to optimize bioleaching conditions for maximum economic competitiveness through design of experiments using iterative response surface methodology (RSM), assisted by thermodynamic modeling. The optimal condition was identified as 2.5% pulp density in 75 mM gluconic acid biolixiviant at 55°C for 30 h which could recover 57%–84% of nickel, 71%–86% of cobalt, and 100% of lithium and manganese, yielding a 17%–26% net profit margin. The recommended pulp density and acid concentrations, together with the observed metal solubilization, were supported by thermodynamic modeling predictions. Our study demonstrated that combining RSM with thermodynamic simulations could be a powerful tool for optimizing bioleaching conditions.

KEYWORDS: Biohydrometallurgy, Steepest ascent method, Ridge analysis, Central composite design, Factorial design, Recycling

1. INTRODUCTION

The production of lithium-ion batteries (LIBs) has increased dramatically because of their superior performance for portable electronic devices and an increase in the demand for electric vehicles. The jump in the use of LIBs means that the quantity of spent batteries will rise significantly in the near future. End-of-life (EOL) LIB stocks have been projected to increase to approximately 1.6 million tonnes in 2030, up from circa 0.3 million tonnes in 2020 (Rajaeifar et al., 2022). Recycling of spent LIBs is critical from both environmental and economic standpoints. The most widely used LIB cathodes including nickel manganese cobalt (NMC) and lithium cobalt oxide (LCO) contain high concentrations of heavy metals that if not properly treated could be harmful to the environment. Additionally, recycling can contribute to sustainable supplies for critical metals such as lithium and cobalt for which demand is expected to outstrip supply (Xu et al., 2020).

Pyrometallurgical recycling is the primary method adopted by industry to recover metal alloys from EOL LIBs. However, lithium is usually lost in the slag (Alipanah et al., 2021), and the required elevated temperatures (900 – 1500˚C) are associated with high energy costs and carbon dioxide emissions (Kwon and Sohn, 2020). Hydrometallurgical approaches are less energy-intensive and can potentially recover a wider variety of metals. Numerous studies have attempted to recover value from EOL LIBs by leaching with mineral acids (Cheng et al., 2019; Gao et al., 2019; Ghassa et al., 2021; Xie et al., 2020). This approach can achieve high efficiency, but harmful gas emissions (e.g., Cl_2 and SO_3) can have adverse effects on the environment and human health (Alipanah et al., 2021). Acid waste generation and the associated high costs for disposal further limit the sustainability of mineral acid based leaching approaches (Xiang et al., 2010).

Biohydrometallurgy is a subfield of hydrometallurgy that has the potential for reduction in chemical and energy consumption (Heydarian et al., 2018). Bioleaching, one of the applications within biohydrometallurgy, is promising because it does not require the addition of toxic chemicals or harsh operating conditions (e.g., high temperature and high pressure)(Asghari et al., 2013; Villares et al., 2016). Instead, the natural ability of microorganisms to produce acidity is harnessed. The most well-established bioleaching approach takes advantage of sulfur and iron oxidizing bacteria to produce sulfuric acid and ferric iron (an oxidant), but organic acids can also be produced by microbes and used for leaching of non-sulfidic feedstocks (Fujita et al., 2022). In the study reported here, cathode-containing powder extracted from pre-processed EOL LIBs, called black mass, was leached with a mixture of organic acids (mainly gluconic acid) produced by the bacterium *Gluconobacter oxydans* (Reed et al., 2016). The biolixiviant was produced by the bacteria from an agricultural waste, corn stover, and the leaching was conducted with ferrous iron addition to reduce and help solubilize the metals.

While bioleaching offers potential environmental benefits, it has not been widely evaluated for recycling EOL LIBs because of recognized challenges. Bioleaching of industrial wastes was often performed at low pulp densities (e.g., ≤1% w/v such as (Zeng et al., 2013)(Biswal et al., 2018)(Mishra et al., 2008)(Xin et al., 2016)(Bahaloo-Horeh et al., 2018)(Bahaloo Horeh et al., 2016)) because recovery efficiency has been observed to decrease with increasing pulp density, due to the presence of alkaline wastes that consume the biologically produced acids or metal toxicity to the microorganisms (Niu et al., 2015; Pathak et al., 2017). Low pulp densities mean larger volumes of lixiviant must be produced and handled, which increases costs. Accordingly, several recent studies tried to explore bioleaching of spent LIBs in higher pulp densities. (Roy et al., 2021) investigated the bioleaching of LCO-based LIB black mass via *A. ferroxidans* produced sulfuric acid at a 10% pulp density with replenished leached liquor that contains a fresh bacterial culture every 24 h for three cycles (i.e., 72 h). (Do et al., 2022) also suggested a 10% pulp density similar to bioleaching process described in (Roy et al., 2021) but with 2 h replenishment cycle

rather 24 h. (Naseri et al., 2023) proposed a LIB bioleaching process via molasses medium by *Penicillium citrinum* at a 7% pulp density. High leaching efficiencies for lithium and manganese were achieved after 6 days of leaching. Bioleaching studies typically report much longer leaching times (e.g., multiple days to weeks) compared to abiotic leaching, further diminishing the economic viability for industry adoption. Understanding how to optimize bioleaching conditions, including pulp density and leaching duration, is a research gap that must be addressed in order to improve the economic viability and prospects for industrial adoption of this new biotechnology.

Most of the existing literature on value recovery from spent LIBs has emphasized maximizing metal recovery efficiencies, but the approach does not necessarily ensure optimal economic returns. For example, one may use large amounts of acid to facilitate metal extraction, but an economically conscious process would consider both resource consumption and leaching efficiency for a more balanced solution. Maximizing metal recovery efficiency may maximize the revenue, but the required expenses may be higher than the income generated, making the process economically infeasible. Table S-1 in Supporting Information summarizes several recent studies that focused on maximizing LIB metal recovery efficiency using design of experiment (DOE), neglecting the process costs.

Factorial design is the most frequently employed DOE approach for studying the leaching of LIB materials because it allows for the screening of factors and the modeling of the relationship between independent variables and their interactions with the response variable (using a first-order model) (Alipanah et al., 2021). A more complex technique known as response surface methodology (RSM) tries to maximize the response by employing a sequential strategy that may include several procedures (e.g., factorial design, steepest ascent or descent, central composite design for second-order models). Several reported RSM studies have used built-in optimizer functions in Minitab or Design Expert software to quickly find the 'optimal' condition in a single run of DOE (Esmaeili et al., 2020; Golmohammadzadeh et al., 2017; Roshanfar et al., 2019).

The objective of the current study is to maximize the net present value (NPV) of the proposed bioleaching process using RSM, aided by thermodynamic modeling. Thermodynamic modeling, specifically aqueous geochemical equilibrium modeling, is an underutilized tool in bioleaching studies but can offer significant benefits (Fujita et al., 2022). Predictions of the equilibrium aqueous solubilities of metals given the temperature and chemical composition of the system can help to constrain the range of parameter values for testing, and lead to more efficient hydrometallurgical process development. A major reason for the infrequent application of such modeling is that it is challenging to construct and parameterize a thermodynamic model in complex systems that include incompletely characterized components (e.g., microbial metabolites, heterogeneous solids). Nevertheless, simplified models based on reasonable assumptions can provide critical guidance in designing and optimizing conditions for leaching. They can also offer insight into the mechanisms underlying the observed results, and a basis for studies of leaching kinetics. For our study, thermodynamic modeling validated one of the important basal conditions for leaching (the provision of ferrous iron in a 1:1 stoichiometric ratio to the active metals Co+Ni+Mn), and supported selection of bioleaching conditions for testing. Figure 1 shows an overall schematic of our approach. The first set of experiments, assuming ferrous iron addition, was designed based on fractional factorial design, where the key design variables (i.e., leaching temperature, pulp density, leaching time, and acid concentration), and their levels were determined based on previous experimental results as well as consideration of the literature. Bioleaching experiments were conducted under the designed conditions, and the measured recovery efficiencies for lithium, cobalt, manganese, and nickel were used as inputs to a techno-economic analysis (TEA) model. The TEA model of (Alipanah et al., 2023) was directly applied to estimate the costs and revenues for each experimental condition to derive the NPV. The NPV served as

the response variable to evaluate the economic performance of bioleaching. Statistical models were developed to estimate the influence of each design variable on the NPV and to predict the 'best' path to improve the NPV. Follow-up experiments were conducted to evaluate the recommended path. Finally, based on the results and additional thermodynamic insights, a new set of experimental designs was developed to further optimize the bioleaching conditions. This iterative process ultimately identified the most promising operational conditions for economic returns.

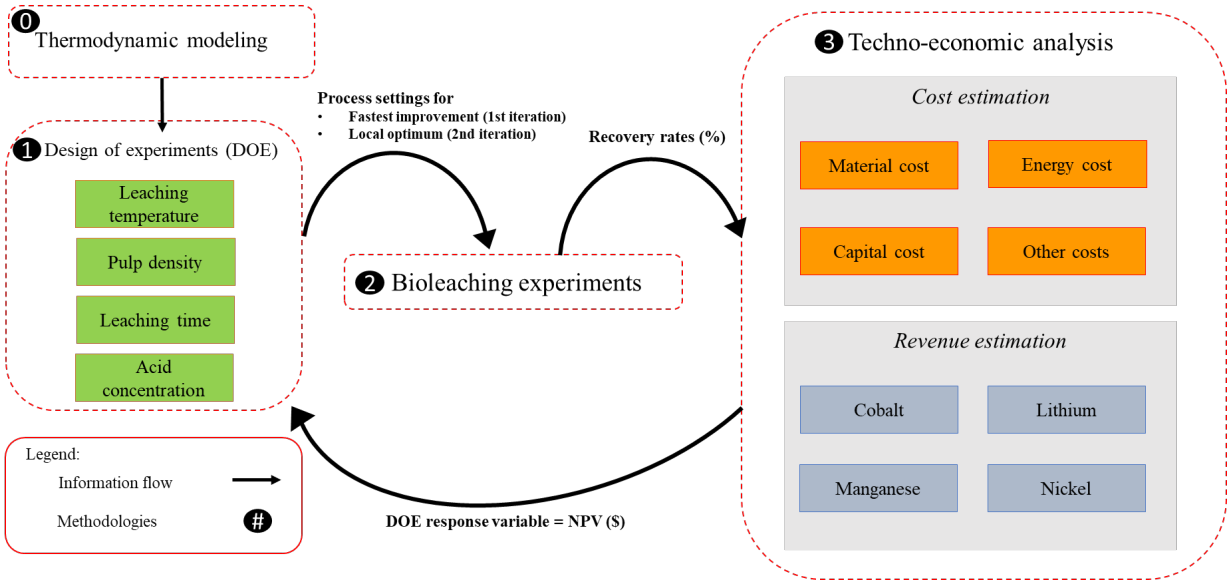

Figure 1. The information flow between thermodynamic modeling, design of experiments, bioleaching experiments, and techno-economic analysis for iterative optimization of bioleaching.

2. MATERIALS AND METHODS

Optimization of the LIB bioleaching process began with experiments using pure $LiCoO_2$ (LCO) cathode powder due to its ease of accessibility, high-value Co content, and more consistent chemistry (enabling thermodynamic modeling) compared to "black mass," a more realistic starting material for LIB recycling. Black mass is typically obtained by mechanical treatment (e.g., crushing, magnetic separation, and sieving) of different EOL LIBs and contains a mixture of cathode and anode materials (Ekberg and Petranikova, 2015). Table S-2 shows the composition of the LCO and particular black mass used in this study. Through the initial experiments with LCO powder, important bioleaching conditions were identified and a path towards accelerated discovery of the improvement direction was identified. Then the feedstock was switched to the more complex black mass, as the ultimate research target was to improve bioleaching conditions for value recovery from a real-world feedstock for LIB recycling.

2.1. Bioleaching

Biolixiviant production: Gluconobacter oxydans strain B58 (received from the Agriculture Research Service, USDA (Peoria, IL), as shown in Reed, et. al., 2016) was grown on corn stover hydrolysate (hot water pretreated and enzymatically hydrolyzed to produce glucose (28 g/L)) in Pikovskaya phosphate

modified (Pkm) medium at 30°C with shaking at 150 rpm for 42 h. The biolixiviant was then harvested by centrifuging the culture to remove the cells and filter (0.22 µm) the supernatant (Jin et al., 2019).

Leaching procedure: DOE bioleaching experiments were conducted with 1 to 18% (w/w) $LiCoO_2$ (MTI Corp, Richmond, CA) or cathode black mass (provided by Retriev Technologies, now Cirba Solutions) added to filtered (0.22 µm) biolixiviant. The dominant biolixiviant organic acid, gluconic acid (82 mM, pH 2.23, from corn stover), was diluted with water or supplemented with commercial gluconic acid (Sigma-Aldrich) to obtain final concentrations ranging from 11 to 228 mM. Leaching temperatures were set at values between 25 and 65°C and leaching durations between 5 and 36 h were tested. Initial biolixiviant pH varied between pH 2.48 and 2.80; the pH was not adjusted prior to contact with the LCO or black mass. Samples (10 mL) were incubated in sealed flasks on an orbital shaker. Each processing condition was replicated 3 times, unless otherwise specified. Bioleachate was collected immediately upon reaching the designating leaching time by centrifugation (10,000 x *g*; 10 min) and filtration (0.22 µm pore size; Millex GP).

Glucose and gluconic acid content were determined by high performance liquid chromatography (HPLC) (Reed et al., 2016)(Thompson et al., 2018). Metal concentrations were determined by atomic adsorption spectroscopy (AAS; Agilent 240FS 200 Series) using acetylene and nitrous oxide with calibration standards for Li, Ni, Co, & Mn (5 mg/L). The samples were diluted in HCl (3%) and the data was analyzed using SpectraAA software.

Iron sulfate as reductant: Ferrous sulfate was added as a reductant to help with metal solubility in the biolixiviant. The beneficial effect of a reducing agent in hydrometallurgical recycling of spent LIB materials and the relevant reactions have been reported by others (Liang et al., 2021)(Ghassa et al., 2020)(Diaz et al., 2020), and were rationalized by the modeling presented in this study. The molar amount of Fe(II) added was determined based on a 1:1 stoichiometry with the estimated total molar content of [Co+Ni+Mn] in the black mass or LCO.

2.2. Thermodynamic modeling

Hydrometallurgical recycling of spent LIB cathode materials under acidic conditions and in the presence of a reducing agent (shown here as iron) involves the dissolution of the metal oxides as shown in Eq.1:

$$LiNi_xMn_yCo_zO_2 + Fe^{2+} + 4H^+ \rightarrow Li + +XNi^{2+} + YMn^{2+} + ZCo^{2+} + Fe^{3+} + 2H_2O \qquad \textbf{Eq.1}$$

where $x + y + z = 1$.

As noted previously, because of the variable chemistry (changing content of Ni, Co and Mn) in the black mass, thermodynamic modeling was conducted using the assumption of LCO as the metal oxide (therefore in equation (1), $x = 0$, $y = 0$, and $z = 1$). Solubilities of Li and Co in the LCO bioleaching system were evaluated using the Mixed-Solvent Electrolyte (MSE) model (Wang et al., 2006; Wang et al., 2002; Wang et al., 2004) as implemented in the OLI Studio software (OLISystems, 2021). The MSE model has been selected because it simultaneously represents phase equilibria (in particular, solid solubilities) and solution speciation including acid-base, complexation, and redox equilibria. The MSE model was constructed by combining an equation of state for standard-state properties of individual species, an excess Gibbs energy model, and an algorithm for solving phase and chemical equilibria in multicomponent and, if necessary, multiphase systems. The model has been systematically verified for various classes of inorganic components such as chlorides (Das et al., 2017; Gruszkiewicz et al., 2007), sulfates (Das et al., 2019), phosphates (Wang et al., 2004) and organic complexing agents (Fujita et al., 2015; Fujita et al., 2020). MSE has been previously validated for applications that share common

characteristics with the bioleaching system studied here, i.e., for solubilities in microbiological media (Fujita et al., 2015), leaching of metals from waste materials (Antonick et al., 2019) and redox transformations combined with solubility behavior (Wang et al., 2017).

The key feature of the thermodynamic simulation is the simultaneous modeling of all reactions and phase equilibria that are important in the leaching process. The model includes the following classes of equilibria:

(i) Acid-base and redox self-dissociation of water.
(ii) Cation hydrolysis and associated solid hydroxide formation for the main cations that participate in the leaching process (i.e., cobalt in both +2 and +3 oxidation states, iron in +2 and +3 oxidation states and lithium) and the cations that originate from the Pkm medium (i.e., Mn, Mg and Ca).
(iii) Solid-liquid equilibria for the dissolution of $LiCoO_2$.
(iv) Aqueous speciation of gluconic acid and gluconate ions.
(v) Aqueous speciation of the inorganic anions that are introduced with the Pkm medium or added with $FeSO_4$ (i.e., sulfate and phosphate ions).
(vi) Complexation equilibria between gluconic acid and all cations that are present in the system. These cations include transition metals and alkaline earth metals, both of which form multiple gluconate complexes.
(vii) Formation of gluconate salts of various cations, which may occur at higher concentrations of either the cations or gluconate ions.
(viii) Cation redox equilibria, which link the different oxidation states of iron and cobalt.
(ix) Aqueous speciation equilibria and associated solid-liquid equilibria for metal sulfates and phosphates, which need to be included because of the presence sulfate and phosphate ions in combination with the cations.

The reactions are specified in detail in Table S-3. The model can be easily extended by including nickel and other metals for simulating the dissolution of multicomponent oxides beyond the base $LiCoO_2$ composition. It should be noted that the equilibrium expressions for the reactions are solved simultaneously because they are inherently interconnected. As a result, equilibrium composition of the system is obtained for given feed conditions. This includes detailed speciation in the aqueous phase and the amounts of solid phases that are in equilibrium with the aqueous phase.

Although experimental solubility data for LCO have not been directly measured, thermochemical properties are available from comprehensive thermochemical measurements (Gotcu-Freis et al., 2015; Jankovsky et al., 2016; Kawaji et al., 2002; Wang and Navrotsky, 2005a, b) and have been used in the model. This is a generally used approach for solids that are sparingly soluble and, in particular, those that undergo incongruent dissolution. Similar data are not available for black mass due to its heterogeneity, and therefore the modeling was limited to the LCO; nevertheless, the predictions generated by the model for LCO were instructive for black mass. The LCO was presumed to be contacted with the microbiological medium (Pkm) in the presence of gluconic acid, which exhibits chelation behavior in addition to impacting the pH; complexation of metals by gluconic acid was included in the modeling. Details of the computations are described in the Supporting Information, section S1.

2.3. Process optimization

To optimize bioleaching technology for value recovery from LIB black mass, four variables were considered (i.e., leaching temperature, pulp density, leaching time, and gluconic acid concentration) for optimization through RSM. Preliminary experiments showed that all four variables have a substantial effect on the leaching efficiency, which determines the revenue generation. From the cost perspective,

pulp density and gluconic acid concentration directly affect material consumption (i.e., acid and water) as well as other cost components such as capital, energy, and labor costs, as they affect the leachate volume to be processed. Leaching time and temperature affect the capital cost and energy cost: For example, the longer leaching time, the larger bioreactor, and the higher energy cost. Based on the modeled impact of the four variables on the economic feasibility through a TEA (please see Figure S-7 for mass-energy balance and refer to (Alipanah et al., 2023) for further details), NPV has been set as the response variable to be maximized. As the experiments involved two LIB feedstocks (i.e., initially LCO cathode and then black mass) whose availabilities are different, the TEA model assumed two hypothetical plants with the processing capacity of 1,000 t/y of LCO cathode and 10,000 t/y of black mass over 30 years. For further information on the NPV estimation, please refer to (Alipanah et al., 2023).

2.3.1. Response surface methodology

Response surface methodology (RSM) is a DOE method to model and analyze a desired response (i.e., NPV in this study) as a function of several variables or factors (i.e., bioleaching conditions). RSM is an efficient tool to continuously improve chemical processes through an iterative application to find the optimal setting. According to Taavitsainen (Taavitsainen, 2012), the optimization process can be summarized as a four-step algorithm: (1) developing an experimental design centered on the current optimal point (or the best guess at first), (2) statistical model fitting, (3) calculation of the gradient path, and (4) conducting experiments along the gradient path as long as the results improve. This four-step procedure should be repeated until no significant improvement is warranted. Typically, a (fractional) factorial design with an optional center point is used first with the assumption that the surface within the design area is approximately linear at the start of the optimization (Taavitsainen, 2012). The additional center point is used to check possible curvature in the design. If the curvature is found to be statistically significant, the design should be upgraded to a second-order design (e.g., central composite design). The following subsections explain each design characteristic.

2.3.1.1. Factorial design

Experimental design. Factorial design considers all possible combinations of pre-determined factor levels for each design variable to formulate their linear effects as well as interaction effects on the response variable. Two-level factorial design (2^N) is the most widely adopted model since it requires fewer experiments than higher-level designs and provides valuable insights about the correlations between factors and the response variable. Each variable has two levels coded as +1 and –1 in this scheme. Eq. 2 shows the coding formula for quantitative variables, where X_i denotes the coded value of the i'th variable, x_i denotes the original value, $\overline{x_i}$ denotes the average value of the two x_i's, and Δx_i denotes the difference between the two x_i values.

$$X_i = \frac{x_i - \overline{x_i}}{\frac{1}{2}\Delta x_i} \quad \textbf{Eq.2}$$

A response y can be formulated as Eq.3 in a factorial design where b_i shows the factor's impact on the response variable.

$$y = b_0 + \sum_{i=1}^{N} b_i X_i + \sum_{i=1}^{N-1} \sum_{i<j}^{N} b_{ij} X_i X_j + \ldots + b_{1,2,\ldots N} X_1 X_2 \ldots X_N \quad \textbf{Eq.3}$$

Gradient path. To identify the steepest ascent, also called gradient path, that would yield the fastest improvement in the response variable, the gradient vector of the fitted model ∇ should be calculated. The next experimental conditions are selected on the gradient path using the scaling factor c (Eq.4). The starting point X_0 is typically the center of factorial design.

$$X_i = X_{i-1} + c\frac{\nabla}{\|\nabla\|} \quad \textbf{Eq.4}$$

The bioleaching optimization started with a half fractional factorial design (2^{4-1}) for LCO material with 3 replications for each experimental condition to identify the steepest ascent for NPV maximization. Table S-5 shows the levels of the considered experimental variables. Because of the costs associated with heating reactors, we chose to stay close to room temperature and typical *G. oxydans* growth conditions (30°C). The gluconic acid concentrations selected for testing were 70 and 95 mM, lower than used in previous experiments (e.g., Figure S-6) due to the anticipated costs of gluconic acid but also bracketing the range identified as optimal (for a pulp density of 1.5%) by thermodynamic modeling which is discussed in section 3.1. For the pulp density, because of previous findings that low pulp densities posed such a significant challenge for economic LIB metal recovery (Thompson et al., 2018), we chose to test higher values (12% and 17.5%) compared to typical bioleaching studies (Table S-1). In our leaching configuration, we do not contact the metal containing solids with active microbial cells, so metal toxicity is not an issue. Although thermodynamic modeling suggested that in our test range of gluconic acid concentrations, the solubility of Co(II) should be limited as pulp densities increase above ~1.5% (Figure S-5a shows the relevant simulation for 80 mM gluconic acid), because of the significant economic benefit of using higher pulp densities, we decided to test whether at shorter leaching times (< 1 day) kinetics might work in our favor. Specifically, we hoped that the precipitation of extracted Co(II) would be slow compared to the reactions leading to dissolution of the LCO, and therefore we could capture the extracted Co if we separated the solid and liquid phases before significant Co(II) precipitation occurred. The results of experiments and the subsequent gradient path are described in section 3.2.

2.3.1.2. Central composite design

Central composite design (CCD) is one of the most common approaches to develop a second-order model. It is composed of a factorial design plus axial or star points (i.e., points with α distance from the center of the design region), and a center point. Eq.5 shows an example of a second-order model derived from a two-variable CCD.

$$y = \beta_0 + \beta_1 X_1 + \beta_2 X_2 + \beta_{12} X_1 X_2 + \beta_{11} {X_1}^2 + \beta_{22} {X_2}^2 \quad \textbf{Eq.5}$$

In order to identify the gradient path from CCD, the stationary point is identified by taking derivatives of the second-order model with respect to each variable and setting the derivatives to zero (Eq.6). The obtained values are fed into the second-order model (e.g., Eq.5) to estimate the predicted response. The second-order model can also be expressed in the form of a Hessian matrix $\hat{B}$ given as Eq.7. To identify whether the stationary point represents the minimum, maximum, or saddle point, the eigenvalues of the matrix $\hat{B}$ are analyzed. If all the eigenvalues are negative, the stationary point is a maximum; if all are positive, the stationary point is a minimum, and if there are different signs in eigenvalues, the point is a saddle point.

$$\frac{\partial y}{\partial X_i} = 0, \ \forall i \in I: Set\ of\ variables \quad \textbf{Eq.6}$$

$$\hat{B} = \begin{bmatrix} \beta_{ii} & \frac{\beta_{ij}}{2} & \frac{\beta_{ik}}{2} \\ \frac{\beta_{ij}}{2} & \beta_{jj} & \frac{\beta_{jk}}{2} \\ \frac{\beta_{ik}}{2} & \frac{\beta_{jk}}{2} & \beta_{kk} \end{bmatrix} \quad \textbf{Eq.7}$$

CCD was applied to bioleaching by setting the center point as the best bioleaching condition identified from the gradient path of the first-order model. As the specific CCD design is dependent on the results from the gradient path analysis, the bioleaching CCD was fully described in section 3.3.

2.3.1.3. Ridge analysis

Ridge analysis (RA) is steepest ascent applied to second-order models where a stationary point is projected to be outside of the experimental region, or the stationary point is identified as a saddle point (Gramacy, 2020). To perform RA, Eq.8 should be solved for different values of μ, starting with the largest eigen value of the matrix $\hat{B}$ for a maximization problem.

$$\left|\hat{B} - \mu I\right|[\boldsymbol{X}] = -\frac{\mathbf{1}}{\mathbf{2}}[\boldsymbol{b}] \qquad \textbf{Eq.8}$$

Where b is a matrix containing coefficients of linear terms in the response equation (Eq.5). The choice of μ is based on the following criteria: $\mu \geq$ maximum eigenvalue of the matrix $\hat{B}$ to get the maximum response which applies to the current study, and $\mu \leq$ minimum eigenvalue of the matrix $\hat{B}$ if we wish to get the minimum response. Then the optimal processing condition X is explored under constrained areas of radius R from the center of design region (Eq.9). We examine adaptive values of μ based on the evenly-spaced grid of R values to find the optimal value of response variable (Gramacy, 2020).

$$\boldsymbol{R} = \sqrt{\boldsymbol{X^T X}} \qquad \textbf{Eq.9}$$

For optimization of bioleaching, RA was applied to the second-order model derived from the CCD. The specific RA and its result were described in section 3.3.

3. RESULTS AND DISCUSSION

3.1. Initial validation of ferrous iron requirement and consideration of gluconic acid concentration

In the absence of ferrous iron addition, solubilization of Co from LCO by leaching with biologically produced gluconic acid was minimal; upon addition of ferrous sulfate at a 1:1 molar ratio of Fe:Co, the extraction of Co into the aqueous phase improved significantly. Figure S-6 shows bioleaching results after leaching LCO (1.5% pulp density) for 24 h at 30°C with 100 mM gluconic acid. Co recovery improved from <10% in the absence of Fe(II) to >60% with Fe(II) addition. These experimental observations were consistent with thermodynamic simulations. In the absence of a reducing agent such as ferrous sulfate, in a system with 1.5% pulp density, essentially all of the Co was predicted to remain in solution at 30°C (Figure S-1) between pH 2 and 10, where the pH was controlled primarily by the gluconic acid concentration. This was because the LCO was predicted to dissolve incongruently, i.e., although the LCO actually starts dissolving in the presence of low concentrations of gluconic acid, in the examined pH range virtually all of the Co(III) is re-precipitated as $Co(OH)_3$ (Figure S-2). The modeling indicated that to achieve significant Co solubility, a reducing agent, in this system $FeSO_4$, needed to be supplied in at least a 1:1 stoichiometric ratio with the Co(III) in order to reduce it to the more soluble Co(II) form (Figures S-3a and S-3b). This stoichiometric Fe(II) addition was presumed for all subsequent simulations.

In addition to the analysis of the requirement for a reducing agent, for the condition of 1.5% pulp density, the modeling indicated that for Co to be completely solubilized, the gluconic acid concentration should be at least approximately 80 mM (Figure S-3b). Examination of Figure S-3b however also suggests that a large excess of gluconic acid would enhance the solubilization of Fe(III), which would otherwise remain in the solid phase as $Fe(OH)_3$, as shown in Figure S-4. Since the formation and maintenance of solid $Fe(OH)_3$ would be more convenient for downstream separations (avoiding the need to separate Fe and Co in the leachate), a gluconic acid concentration close to the minimum necessary for solubilization of Co would be advantageous.

3.2. First-order model

Fractional factorial design: Table S-6 shows fractional factorial design and the experimental results, i.e., the measured Co recovery efficiency, and calculated NPVs. Unfortunately, the initial design yielded low levels of Co recovery (< 20%) and negative NPVs for all tested conditions It was found that NPV is heavily influenced by temperature, pulp density, and time (Figure S-8). More details on the fitted first-order model are shown in Table S-7: Analysis of variance (ANOVA). The results indicated the need for a significant improvement through the next step of RSM, which was the identification of a gradient path.

Gradient path: Conditions along the gradient path (Table S-8) were determined by taking the first-order derivative, as shown in Eq. 4. Two-way interactions were disregarded as they were statistically insignificant, as shown in Table S-7. The two most significant variables were temperature and pulp density. Figure 2(a) shows the gradient path and the results that indicated that decreasing pulp density and increasing leaching temperature would improve the NPV of bioleaching LCO. The impetus toward decreasing pulp densities (from >12%) was consistent with the thermodynamic modeling predictions, meaning that under these conditions the kinetics, i.e., the balance between the rates of dissolution and re-precipitation of the extracted Co, were not in our favor. The simulations shown in Figure S-5a predicted that with 80 mM gluconic acid at 30°C, increasing fractions of the Co(II) would precipitate as a $Co(OH)_2$ phase, as pulp densities rose above 1.5%.

As for the effect of temperature, the thermodynamic simulations predicted that a very slight increase in equilibrium Co solubility would be associated with increased temperature (Figure S-5b shows the simulation for 80 mM gluconic acid at 60°C; appreciable $Co(OH)_2$ precipitation does not appear until the pulp density exceeds ~1.8%). In the physical experiments the improvement in metal solubilization observed at higher temperatures was significant (Table S-8 includes the experimentally measured Co recoveries and calculated NPVs). Again, the actual observed Co solubility, prior to reaching equilibrium, is dependent on the relative kinetics of dissolution and precipitation of competing Co containing phases. A similar trend of increasing metal solubilization with decreasing pulp density and increasing temperature was observed when the LIB feedstock was switched from LCO cathode material to black mass and an additional 7 experiments were conducted along the same gradient path, as shown in Figure 2(b). The figure shows that NPV would not improve after performing experiment G-6. Therefore, experiment G-6 was set as the center point of the next experimental design, and a full factorial design was developed around the conditions associated with G-6 (60°C, 3.5% pulp density, 30 h, 72 mM gluconic acid). The resulting ANOVA showed the significance of curvature around that point with *p-value* < 0.05 (Table S-9), so we upgraded the design to a second-order design by adding axial points to the existing full factorial design to build a CCD.

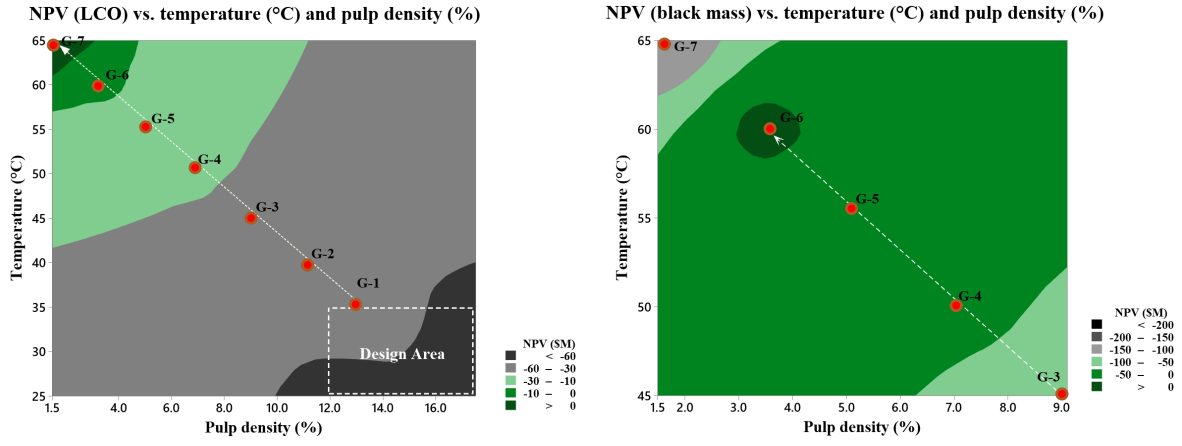

(a) **(b)**

Figure 2. Contour plots showing the gradient paths derived from the fractional factorial design. (a) Contour plot of LCO cathode bioleaching. The white rectangle shows the initial design region. The white dashed arrow shows the gradient path. (b) Contour plot of black mass bioleaching.

3.3. Second-order model

Central composite design: Table 1 shows the CCD and the measured metal recovery efficiencies from the physical experiments. Eq. S-1 shows the second-order model fitted on the experimental results derived from CCD. The coefficient of determination (R^2) was 86%, indicating adequate fit from the experimental data (i.e., only 14% of variation in NPV not explained by the model). The adjusted coefficient of determination ($R^2(adj)$) was 83%, confirming the model significance (please see Table S-10 for the ANOVA). The profitability of the process is mostly dependent on pulp density and its quadratic and interaction effects (Figure S-9). Lower pulp densities could provide higher revenue with higher metal recovery efficiencies (e.g., compare experiment #1 vs. experiment #3 in Table 1), but they impose

significantly higher processing costs and reduce NPVs. Higher pulp densities require lower volumes of leachate to process the same amount of black mass, lowering all of the associated costs.

Table 1. Central composite design for bioleaching of black mass, metal recovery efficiencies (3 replications for factorial and star points, 5 replications for the center point), and associated average NPVs. Experimental condition #18, highlighted in bold, shows the highest NPV.

No.	Point type*	A temperature (°C)	B: pulp density (%)	C: time (h)	D: gluconic acid concentration (mM)	Li recovery (%)	Co recovery (%)	Mn recovery (%)	Ni recovery (%)	NPV ($ M)
1	F	55	1	24	50	100, 100, 100	57, 65, 72	100, 90, 100	62, 65, 95	-58.6
2	F	65	1	24	50	100, 100, 100	77, 36, 34	100, 96, 77	83, 22, 12	-187.7
3	F	55	4	24	50	100, 100, 100	55, 53, 57	80, 84, 89	44, 58, 66	31.1
4	F	65	4	24	50	100, 100, 100	50, 59, 53	84, 99, 84	52, 67, 55	25.9
5	F	55	1	36	50	100, 100, 100	38, 52, 68	99, 100, 100	15, 47, 100	-148.5
6	F	65	1	36	50	100, 100, 100	33, 31, 32	100, 100, 100	20, 12, 22	-329.7
7	F	55	4	36	50	100, 100, 100	47, 51, 54	95, 86, 94	43, 57, 60	4.4
8	F	65	4	36	50	100, 100, 100	58, 55, 59	88, 82, 99	54, 50, 58	32.0
9	F	55	1	24	100	100, 100, 100	37, 57, 51	100, 95, 86	43, 43, 40	-279.4
10	F	65	1	24	100	100, 100, 100	38, 39, 36	82, 100, 100	34, 26, 28	-374.4
11	F	55	4	24	100	100, 100, 100	57, 80, 72	100, 98, 87	64, 62, 57	69.1
12	F	65	4	24	100	100, 100, 100	49, 57, 62	94, 100, 92	63, 69, 54	3.3
13	F	55	1	36	100	100, 100, 100	56, 38, 47	100, 100, 100	50, 16, 45	-319.4
14	F	65	1	36	100	100, 100, 100	26, 17, 42	100, 100, 100	12, 1, 32	-457.2
15	F	55	4	36	100	100, 100, 100	76, 61, 62	100, 100, 100	69, 63, 71	62.5
16	F	65	4	36	100	100, 100, 100	63, 66, 53	100, 100, 100	59, 64, 46	21.7
17	C	60	2.5	30	75	100, 100, 100, 100, 100	43, 78, 55, 64, 75, 59	70, 100, 90, 100, 100, 100	31, 65, 47, 67, 70, 40	8.5
18	**S**	**55**	**2.5**	**30**	**75**	**100, 100, 100**	**86, 71, 75**	**100, 100, 100**	**84, 57, 74**	**92.3**
19	S	65	2.5	30	75	100, 100, 100	65, 45, 56	100, 100, 100	81, 88, 75	-22.6
20	S	60	1	30	75	100, 100, 100	79, 53, 42	100, 100, 95	100, 56, 81	-155.3
21	S	60	4	30	75	100, 100, 100	54, 60, 56	100, 95, 90	97, 76, 64	35.3
22	S	60	2.5	24	75	100, 100, 100	66, 60, 63	100, 97, 100	67, 62, 67	19.1
23	S	60	2.5	36	75	100, 100, 100	60, 71, 70	100, 92, 95	53, 68, 70	44.7
24	S	60	2.5	30	50	100, 100, 100	63, 62, 71	92, 96, 92	52, 64, 52	45.1
25	S	60	2.5	30	100	100, 100, 100	63, 79, 90	100, 92, 100	52, 65, 67	56.5

*F: factorial points, C: center of design, S: star points

Using a system of equations shown in Eq.6, the stationary point of the model was projected to be outside of the design region, where the coded acid concentration is 1.2 (i.e., 105 mM) and NPV is $91M. To determine whether the found stationary point represents a minimum, maximum, or saddle point, the eigenvalues of the matrix $\hat{B}$ (Eq.6) were calculated; $\lambda_1 \approx -12*10^7$, $\lambda_2 \approx -23*10^6$, $\lambda_3 \approx -18*10^6$, $\boldsymbol{\lambda_4} \approx 3*10^6$.

Ridge analysis: The mixed signs of eigenvalues revealed a saddle point, so RA was performed to find the best experimental condition that maximizes the NPV. We tested three more experimental conditions with different radii (R-1=1.3, R-2=1.9, R-3=2.4) (Table S-11). RA predicted higher NPVs, as we moved farther away from the center of the design (Figure S-10). However, the confidence interval grows

exponentially, as we move outside of the design region (i.e., R>1), indicating a high uncertainty in bioleaching performance We conducted experiments on the bioleaching conditions suggested by the RA and confirmed that the actual metal recovery efficiencies and NPVs were lower than those of the stationary point from CCD, so we stopped the iterative RSM at this point.

The optimal bioleaching condition: By looking at the surface plot derived from CCD (Figure 3), the best point inside the design region was identified as the optimal point (the first star point in Table 1). That is, the star point setting of A= 55°C, B= 2.5%, C= 30 h, and D=75 mM showed the highest NPV (~$92M) with metal recovery efficiencies of up to 84%, 86%, 100%, and 100% for nickel, cobalt, manganese, and lithium, respectively. To compare our results with other recent bioleaching studies, Table S-12 was provided, showing the bioleaching processing conditions and metal leaching efficiencies. Although this study optimized the process with the goal of maximizing NPV, unlike other studies that focused on maximizing leaching efficiency, substantial metal leaching efficiencies were achieved in a shorter leaching time and higher pulp density than a majority of the other studies.

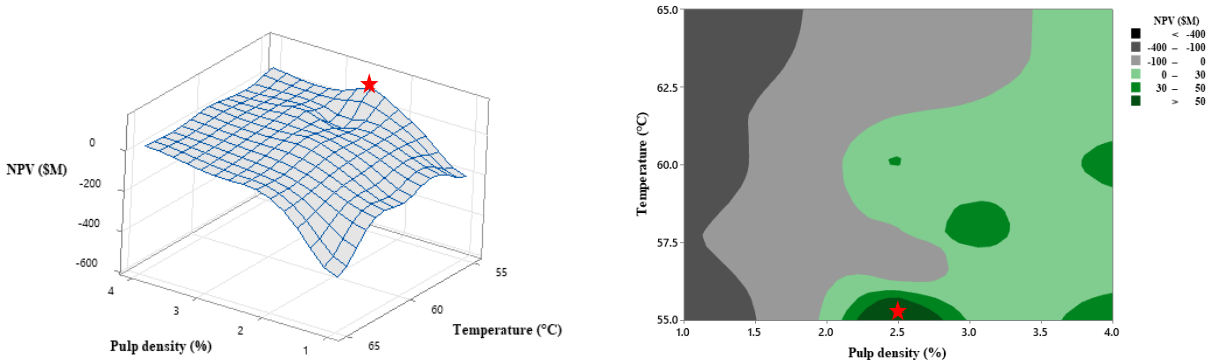

Figure 3. Surface and contour plots of NPV for bioleaching of black mass.

It is striking to note that the thermodynamic simulation of those conditions (i.e., 55°C, pulp density 2.5% and 75 mM gluconic acid) for LCO predicted 77% cobalt recovery and 100% Li recovery at equilibrium. The predicted Co recovery was well within the range of the values for Co and Ni recovery from black mass reported for the experimental condition #18 in Table 1 (Co and Ni would be expected to behave similarly, while Mn speciation and behavior in the black mass system is more complex), and the predicted and measured Li recoveries were identical at 100%. Thermodynamic simulations predicted further that for the selected pulp density and temperature, a gluconic acid concentration of 135 mM would be required to completely solubilize the Co (Figure 4).

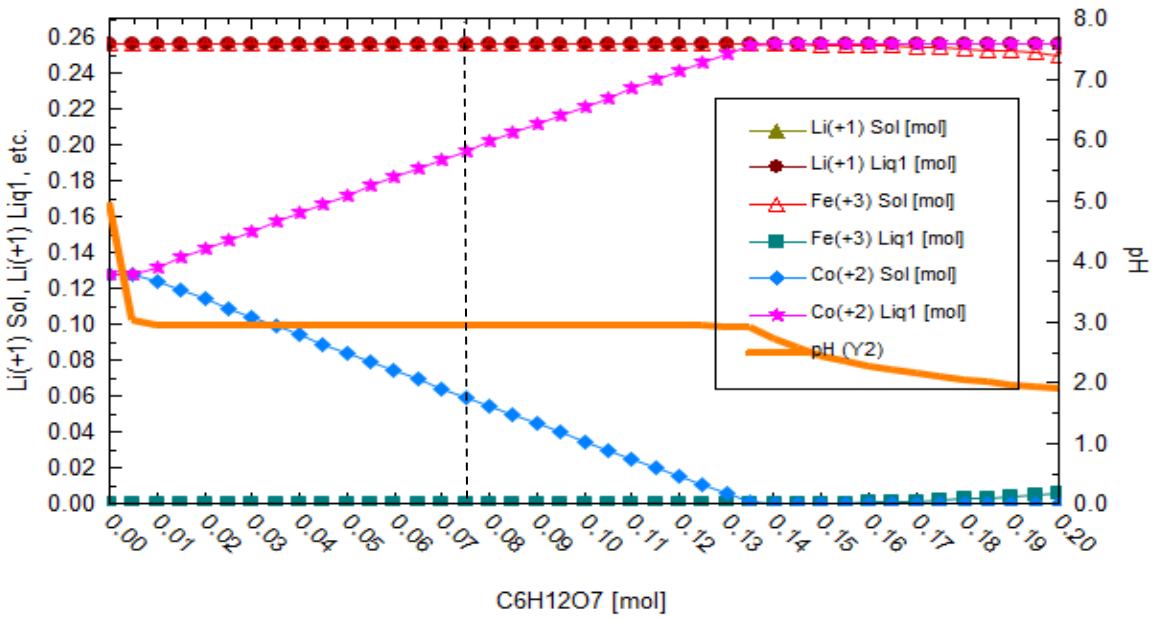

Figure 4. Total concentrations of Li and Co in the aqueous phase and solid phases at a pulp density of 2.5% when $FeSO_4$ is added at a 1:1 molar Co:Fe ratio at 55°C as a function of gluconic acid concentration.

Figure 5 summarizes the overall optimization process of the black mass bioleaching. Experimental conditions G-3 to G-6 show the improvement along the gradient path derived from the first-order model, which was formulated by a fractional factorial design. The final optimal bioleaching condition was found from the second-order CCD model formulated around the best point from the prior gradient path (i.e., G-6). The subsequent RA confirmed no further improvement could be achieved, so our analysis stopped there.

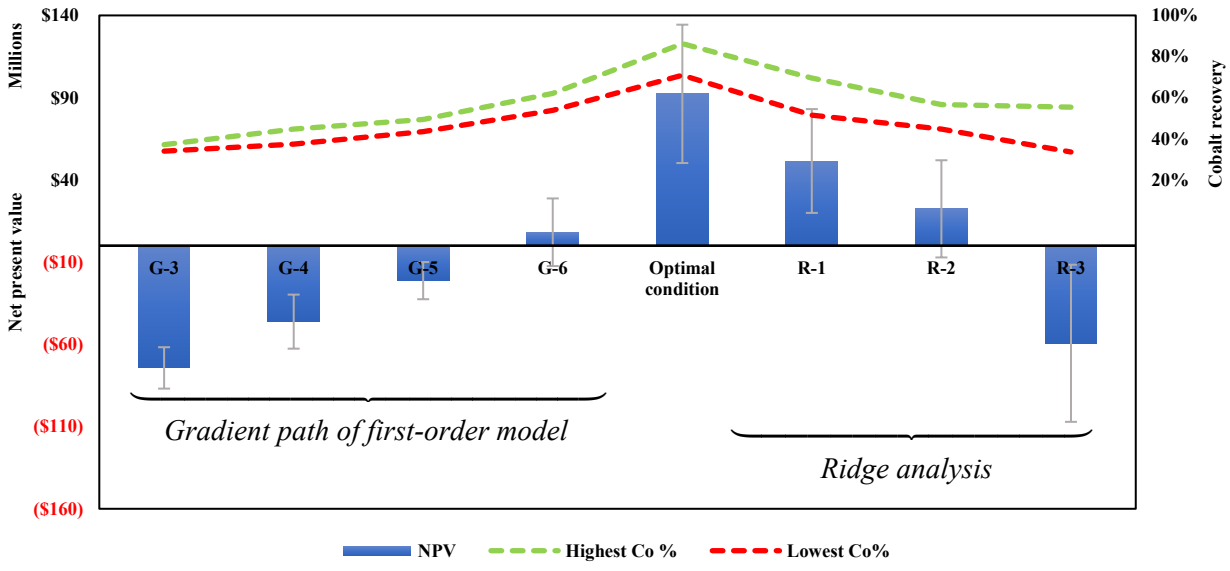

Figure 5. The optimization process through RSM. Blue bars show the estimated average NPV of each experimental condition; the red dashed line shows the lowest achieved cobalt recovery efficiency from 3-5 replications of bioleaching experiments, and the green dashed line shows the highest achieved cobalt recovery efficiency.

4. CONCLUSION

Recycling of spent LIBs is critical for satisfying the increasing demand for critical materials and protecting the environment from hazards posed by discarded batteries as well as mining activities. Bioleaching has promising potential for eco-friendly recycling of LIBs, but the technology has not been commercialized, partly due to its low technology readiness level and uncertain economic feasibility. To help address these challenges, the purpose of this study was to optimize a bioleaching process based on the production of gluconic acid by the bacterium *Gluconobacter oxydans*, with the goal of maximizing its economic prospects and improving the technology readiness level for industrial adoption. The optimization was accomplished through two iterations of RSM assisted by thermodynamic simulations. The simulations provided a thermodynamic foundation for experimental design by predicting the influence of the primary factors that were expected to impact leaching, i.e., gluconic acid concentration and pulp density, and confirmed the requirement for a stoichiometric ratio of $FeSO_4$ to LCO as a reducing agent. Temperature was identified by the modeling as a secondary factor, but the experimental results indicated that the balance between the kinetics of dissolution and precipitation reactions could play an important role. The best bioleaching conditions were identified as leaching temperature of 55°C, pulp density of 2.5%, leaching time of 30 h, and gluconic acid concentration of 75 mM. The measured metal recovery efficiencies from black mass were up to 100% lithium, 100% manganese, 86% cobalt, and 84% nickel. Thermodynamic predictions of the Co recovery from LCO leached under these conditions were remarkably consistent with the observations for the black mass, indicating the value of the simulations and suggesting that at this point the system was approaching equilibrium.

In addition to the utilization of the insights provided by thermodynamic modeling, a unique attribute of this optimization study was that the optimization target was the economic performance of the LIB recycling process rather than the absolute efficiency of metal recovery, as prevalent in the existing literature. Indeed, our thermodynamic simulations suggested that higher gluconic acid concentrations should be used to solubilize all the cobalt. Yet this was not economically optimal. Our approach aims to minimize the processing cost and maximize the revenue for commercialization of a LIB bioleaching technology. We estimated that the proposed bioleaching process could achieve more than $92M of NPV when recycling 10,000 t of black mass per year for 30 years. This finding supports further development of this bioleaching technology.

5. ACKNOWLEDGMENT

We thank Idaho National Laboratory scientists M. Shi for AAS analysis, K. Schaller for HPLC analysis, and L. Aldana Diaz for sharing black mass, a gift from Retriev Technologies (Diaz et al., 2020), as well as the black mass chemical composition data. This research was supported by the Critical Materials Innovation Hub funded by the US Department of Energy, Office of Energy Efficiency and Renewable Energy, Advanced Materials and Manufacturing Technologies Office, which supports early-stage research to advance innovation in U.S. manufacturing and promote American economic growth and energy security. CMI seeks ways to reduce supply risks on rare-earth metals and other materials critical to the success of clean energy technologies. Work is conducted under DOE Idaho Operations Office Contract DE-AC07-05ID14517 and University of Arizona Subcontract number SC-21-556 with the Ames National Laboratory. Accordingly, the U.S. Government retains a nonexclusive, royalty-free license to

publish or reproduce the published form of this contribution, and allow others to do so, for U.S. Government purposes.

REFERENCES

Alipanah, M., Reed, D., Thompson, V., Fujita, Y., Jin, H., 2023. Sustainable bioleaching of lithium-ion batteries for critical materials recovery. J. Clean. Prod. 382, 135274. https://doi.org/10.1016/j.jclepro.2022.135274

Alipanah, M., Saha, A.K., Vahidi, E., Jin, H., 2021. Value recovery from spent lithium-ion batteries: A review on technologies, environmental impacts, economics, and supply chain. Clean Technol. Recycl. 1, 152–184. https://doi.org/10.3934/ctr.2021008

Asghari, I., Mousavi, S.M., Amiri, F., Tavassoli, S., 2013. Bioleaching of spent refinery catalysts: A review. J. Ind. Eng. Chem. 19, 1069–1081. https://doi.org/10.1016/j.jiec.2012.12.005

Bahaloo-Horeh, N., Mousavi, S.M., Baniasadi, M., 2018. Use of adapted metal tolerant Aspergillus niger to enhance bioleaching efficiency of valuable metals from spent lithium-ion mobile phone batteries. J. Clean. Prod. 197, 1546–1557. https://doi.org/10.1016/j.jclepro.2018.06.299

Bahaloo Horeh, N., Mousavi, S.M., Shojaosadati, S.A., 2016. Bioleaching of valuable metals from spent lithium-ion mobile phone batteries using Aspergillus Niger. J. Power Sources 320, 257–266. https://doi.org/10.1016/j.jpowsour.2016.04.104

Biswal, B.K., Jadhav, U.U., Madhaiyan, M., Ji, L., Yang, E.H., Cao, B., 2018. Biological Leaching and Chemical Precipitation Methods for Recovery of Co and Li from Spent Lithium-Ion Batteries. ACS Sustain. Chem. Eng. 6, 12343–12352. https://doi.org/10.1021/acssuschemeng.8b02810

Cheng, Q., Chirdon, W.M., Lin, M., Mishra, K., Zhou, X., 2019. Characterization, modeling, and optimization of a single-step process for leaching metallic ions from LiNi 1/3 Co 1/3 Mn 1/3 O 2 cathodes for the recycling of spent lithium-ion batteries. Hydrometallurgy 185, 1–11. https://doi.org/10.1016/j.hydromet.2019.01.003

Diaz, L.A., Strauss, M.L., Adhikari, B., Klaehn, J.R., McNally, J.S., Lister, T.E., 2020. Electrochemical-assisted leaching of active materials from lithium ion batteries. Resour. Conserv. Recycl. 161, 104900. https://doi.org/10.1016/j.resconrec.2020.104900

Do, M.P., Jegan Roy, J., Cao, B., Srinivasan, M., 2022. Green Closed-Loop Cathode Regeneration from Spent NMC-Based Lithium-Ion Batteries through Bioleaching. ACS Sustain. Chem. Eng. 10, 2634–2644. https://doi.org/10.1021/acssuschemeng.1c06885

Ekberg, C., Petranikova, M., 2015. Lithium Batteries Recycling, Lithium Process Chemistry: Resources, Extraction, Batteries, and Recycling. Elsevier Inc. https://doi.org/10.1016/B978-0-12-801417-2.00007-4

Esmaeili, M., Rastegar, S.O., Beigzadeh, R., Gu, T., 2020. Ultrasound-assisted leaching of spent lithium ion batteries by natural organic acids and H2O2. Chemosphere 254. https://doi.org/10.1016/j.chemosphere.2020.126670

Fujita, Y., Park, D., Lencka, M., Anderko, A., Reed, D., Thompson, V., Das, G., 2022. Beneficiation of REE: Prospects for Biotechnology Deployment. Authorea Prepr. 1–52. https://doi.org/10.1002/essoar.10510876.1

Gao, G., Luo, X., Lou, X., Guo, Y., Su, R., Guan, J., Li, Y., Yuan, H., Dai, J., Jiao, Z., 2019. Efficient sulfuric acid-Vitamin C leaching system: Towards enhanced extraction of cobalt from spent lithium-ion batteries. J. Mater. Cycles Waste Manag. https://doi.org/10.1007/s10163-019-00850-4

Ghassa, S., Farzanegan, A., Gharabaghi, M., Abdollahi, H., 2021. Iron scrap, a sustainable reducing agent for waste lithium ions batteries leaching: An environmentally friendly method to treating waste with waste. Resour. Conserv. Recycl. 166, 105348. https://doi.org/10.1016/j.resconrec.2020.105348

Ghassa, S., Farzanegan, A., Gharabaghi, M., Abdollahi, H., 2020. The reductive leaching of waste lithium ion batteries in presence of iron ions: Process optimization and kinetics modelling. J. Clean. Prod. 262. https://doi.org/10.1016/j.jclepro.2020.121312

Golmohammadzadeh, R., Rashchi, F., Vahidi, E., 2017. Recovery of lithium and cobalt from spent lithium-ion batteries using organic acids: Process optimization and kinetic aspects. Waste Manag. 64, 244–254. https://doi.org/10.1016/j.wasman.2017.03.037

Gramacy, R.B., 2020. Surrogates: Gaussian process modeling, design, and optimization for the applied sciences. Chapman and Hall/CRC.

Heydarian, A., Mousavi, S.M., Vakilchap, F., Baniasadi, M., 2018. Application of a mixed culture of adapted acidophilic bacteria in two-step bioleaching of spent lithium-ion laptop batteries. J. Power Sources 378, 19–30. https://doi.org/10.1016/j.jpowsour.2017.12.009

Jin, H., Reed, D.W., Thompson, V.S., Fujita, Y., Jiao, Y., Crain-Zamora, M., Fisher, J., Scalzone, K., Griffel, M., Hartley, D., Sutherland, J.W., 2019. Sustainable Bioleaching of Rare Earth Elements from Industrial Waste Materials Using Agricultural Wastes. ACS Sustain. Chem. Eng. 7, 15311–15319. https://doi.org/10.1021/acssuschemeng.9b02584

Kwon, O. sung, Sohn, I., 2020. Fundamental thermokinetic study of a sustainable lithium-ion battery pyrometallurgical recycling process. Resour. Conserv. Recycl. 158, 104809. https://doi.org/10.1016/j.resconrec.2020.104809

Liang, Z., Cai, C., Peng, G., Hu, J., Hou, H., Liu, B., Liang, S., Xiao, K., Yuan, S., Yang, J., 2021. Hydrometallurgical Recovery of Spent Lithium Ion Batteries: Environmental Strategies and Sustainability Evaluation. ACS Sustain. Chem. Eng. 9, 5750–5767. https://doi.org/10.1021/acssuschemeng.1c00942

Mishra, D., Kim, D.J., Ralph, D.E., Ahn, J.G., Rhee, Y.H., 2008. Bioleaching of metals from spent lithium ion secondary batteries using Acidithiobacillus ferrooxidans. Waste Manag. 28, 333–338. https://doi.org/10.1016/j.wasman.2007.01.010

Naseri, T., Mousavi, S.M., Liese, A., Kuchta, K., 2023. Bioleaching of valuable metals from spent LIBs followed by selective recovery of manganese using the precipitation method: Metabolite maximization and process optimization. J. Environ. Manage. 343, 118197. https://doi.org/10.1016/j.jenvman.2023.118197

Niu, Z., Huang, Q., Wang, J., Yang, Y., Xin, B., Chen, S., 2015. Metallic ions catalysis for improving bioleaching yield of Zn and Mn from spent Zn-Mn batteries at high pulp density of 10%. J. Hazard. Mater. 298, 170–177. https://doi.org/10.1016/j.jhazmat.2015.05.038

Pathak, A., Morrison, L., Healy, M.G., 2017. Catalytic potential of selected metal ions for bioleaching, and potential techno-economic and environmental issues: A critical review. Bioresour. Technol. 229, 211–221. https://doi.org/10.1016/j.biortech.2017.01.001

Rajaeifar, M.A., Ghadimi, P., Raugei, M., Wu, Y., Heidrich, O., 2022. Challenges and recent developments in supply and value chains of electric vehicle batteries: A sustainability perspective. Resour. Conserv. Recycl. 180. https://doi.org/10.1016/j.resconrec.2021.106144

Reed, D.W., Fujita, Y., Daubaras, D.L., Jiao, Y., Thompson, V.S., 2016. Bioleaching of rare earth elements from waste phosphors and cracking catalysts. Hydrometallurgy 166, 34–40.

https://doi.org/10.1016/j.hydromet.2016.08.006

Roshanfar, M., Golmohammadzadeh, R., Rashchi, F., 2019. An environmentally friendly method for recovery of lithium and cobalt from spent lithium-ion batteries using gluconic and lactic acids. J. Environ. Chem. Eng. 7. https://doi.org/10.1016/j.jece.2018.11.039

Roy, J.J., Madhavi, S., Cao, B., 2021. Metal extraction from spent lithium-ion batteries (LIBs) at high pulp density by environmentally friendly bioleaching process. J. Clean. Prod. 280, 124242. https://doi.org/10.1016/j.jclepro.2020.124242

Taavitsainen, V.-M.T., 2012. Experimental Optimization and Response Surfaces, in: Chemometrics in Practical Applications. pp. 91–138. https://doi.org/10.5772/33265

Thompson, V.S., Gupta, M., Jin, H., Vahidi, E., Yim, M., Jindra, M.A., Nguyen, V., Fujita, Y., Sutherland, J.W., Jiao, Y., Reed, D.W., 2018. Techno-economic and Life Cycle Analysis for Bioleaching Rare-Earth Elements from Waste Materials. ACS Sustain. Chem. Eng. 6, 1602–1609. https://doi.org/10.1021/acssuschemeng.7b02771

Villares, M., Işildar, A., Mendoza Beltran, A., Guinee, J., 2016. Applying an ex-ante life cycle perspective to metal recovery from e-waste using bioleaching. J. Clean. Prod. 129, 315–328. https://doi.org/10.1016/j.jclepro.2016.04.066

Xiang, Y., Wu, P., Zhu, N., Zhang, T., Liu, W., Wu, J., Li, P., 2010. Bioleaching of copper from waste printed circuit boards by bacterial consortium enriched from acid mine drainage. J. Hazard. Mater. 184, 812–818. https://doi.org/10.1016/j.jhazmat.2010.08.113

Xie, J., Huang, K., Nie, Z., Yuan, W., Wang, X., Song, Q., Zhang, X., Zhang, C., Wang, J., Crittenden, J.C., 2020. An effective process for the recovery of valuable metals from cathode material of lithium-ion batteries by mechanochemical reduction. Resour. Conserv. Recycl. 168, 105261. https://doi.org/10.1016/j.resconrec.2020.105261

Xin, Y., Guo, X., Chen, S., Wang, J., Wu, F., Xin, B., 2016. Bioleaching of valuable metals Li, Co, Ni and Mn from spent electric vehicle Li-ion batteries for the purpose of recovery. J. Clean. Prod. 116, 249–258. https://doi.org/10.1016/j.jclepro.2016.01.001

Xu, C., Dai, Q., Gaines, L., Hu, M., Tukker, A., Steubing, B., 2020. Future material demand for automotive lithium-based batteries. Commun. Mater. 1. https://doi.org/10.1038/s43246-020-00095-x

Zeng, G., Luo, S., Deng, X., Li, L., Au, C., 2013. Influence of silver ions on bioleaching of cobalt from spent lithium batteries. Miner. Eng. 49, 40–44. https://doi.org/10.1016/j.mineng.2013.04.021